

# The Role of Gas Disk Gravitational Instability Models in Exoplanet Population Synthesis Models



Alan Boss

Earth & Planets Laboratory, Carnegie Institution for Science, Washington, DC



## Introduction

Results are summarized for an extensive set of three-dimensional hydrodynamics models of the formation of gas giant protoplanets by the gas disk gravitational instability mechanism. The models are intended to be the first steps toward creating a hybrid model for exoplanet population synthesis, where a combination of the core accretion and disk instability mechanisms works in tandem to attempt to reproduce the exoplanet demographics emerging from numerous large surveys, using Doppler spectroscopy, gravitational microlensing, and transit photometry, especially that from space-based telescopes (i.e., Kepler and TESS). Observational evidence supports the formation of massive exoplanets by disk instability around metal-poor stars and on wide orbits, but the present models focus instead on the more controversial question of formation by disk instability inside 20 AU around a protostar with solar metallicity. Boss (2017) presented models that showed the outcome of a phase of disk gravitational instability depends more strongly on the initial conditions adopted for the models than on the assumed disk cooling rate  $\beta$ . The Boss (2019) models then studied the evolution of protoplanetary disks into gravitationally unstable configurations, which is evidently just as important a factor as the disk cooling process. Remarkably, the models have shown that starting from a gravitationally stable, high Toomre Q disk, disks with a large range of cooling rates, from  $\beta = 1$  to 100, eventually become gravitationally unstable, forming numerous spiral arms, and then dense clumps requiring the insertion of virtual protoplanets (VPs) representing newly formed gas giant protoplanets. Models with quadrupled spatial grid resolution compared to that in Boss (2019) have confirmed the viability of the VP approach to modeling dense clumps. These models imply that protoplanetary disks with masses of  $\sim 0.1$  solar masses (e.g., FU Orionis star disks) should be able to form gas giants with initial masses up to  $\sim 4$  Jupiter masses orbiting from  $\sim 4$  AU to  $\sim 20$  AU around a solar-mass protostar. This implies the existence of a largely unseen population of gas giants orbiting solar-type stars, which could be detected by the gravitational microlensing survey and coronagraphic direct imaging technology efforts of the NASA WFIRST space mission, slated for launch around late 2025.

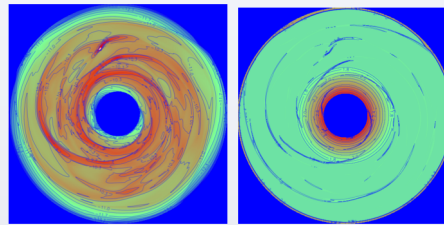
## Numerical Methods and Initial Conditions

The numerical code is the same as that used by Boss (2017, 2019), which can be consulted for further details. The EDTONS code solves the three-dimensional equations of hydrodynamics and the Poisson equation for the gravitational potential, with second-order accuracy in both space and time, on a spherical coordinate grid (see Boss & Myhill 1992). The grid has  $N_r = 100, 200$ , or 400 uniformly spaced radial grid points,  $N_\theta = 23$  theta grid points, distributed from  $\pi/2 \geq \theta \geq 0$  and compressed toward the disk midplane, and  $N_\phi = 512, 1024$ , or 2048 uniformly spaced azimuthal grid points. The radial grid extends from 4 to 20 au, with disk gas flowing inside 4 au being added to the central protostar. The gravitational potential is obtained through a spherical harmonic expansion, including terms up to  $N_{lmax} = 48$  for all spatial resolutions.

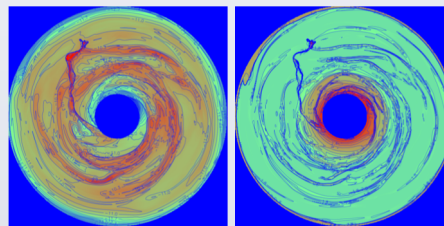
The  $r$  and  $\phi$  numerical resolution is doubled and then quadrupled when needed to avoid violating the Jeans length (e.g., Boss et al. 2000) and Toomre length criteria (Nelson 2006). As in Boss (2017, 2019), if either criterion is violated, the calculation stops, and the data from a time step prior to the criterion violation is used to double the spatial resolution in the relevant direction by dividing each cell into half while conserving mass and momentum. Here, however, the models can be doubled again to as high a spatial resolution as  $N_r = 400$  and  $N_\phi = 2048$  if needed. Even with this quadrupled spatial resolution, in a few models dense clumps formed that violated the Jeans or Toomre length criteria at their density maxima. In that case, the maximum density cell is again drained of 90% of its mass and momentum, which is then inserted into a virtual protoplanet (VP; Boss 2005), as in Boss (2017, 2019). The VPs orbit in the disk midplane, subject to the gravitational forces of the disk gas, the central protostar, and any other VPs, while the disk gas is subject to the gravity of the VPs. VPs gain mass at the rate (Boss 2005, 2013) given by the Bondi-Hoyle-Lyttleton (BHL) formula (e.g., Ruffert & Arnott 1994), as well as the angular momentum of any accreted disk gas. As in Boss (2017, 2019), VPs that reach the inner or outer boundaries are simply tallied and removed from the calculation.

In the Boss (2017, 2019) models, the initial gas disk density distribution is that of an adiabatic, self-gravitating, thick disk with a mass of  $M_d = 0.091 M_\odot$ , in near-Keplerian rotation around a solar mass protostar with  $M_* = 1.0 M_\odot$  (Boss 1993). The initial outer disk temperature was set to 180 K for all models, yielding an initial minimum value of the Toomre (1964) Q gravitational stability parameter of 2.7, i.e., gravitationally stable, though the disks were allowed to cool down to as low as 40 K, as in Boss (2019). Gammie (2001) proposed that the outcome of a gas disk gravitational instability would depend on the parameter  $\beta = t_{cool}\Omega$ , where  $t_{cool}$  is the local cooling time and  $\Omega$  is the local angular velocity of the disk. Gammie (2001) suggested a critical value for fragmentation of  $\beta_{crit} = 3$ . Boss (2017, 2019) discussed the problem of radiative transfer and cooling in disk instability calculations and the utility of the  $\beta$  cooling approximation in sidestepping some of these issues. Boss (2017) described how the  $\beta$  cooling approximation was incorporated into the solution of the specific internal energy equation (Boss & Myhill 1992), where the time rate of change of energy per unit volume, which is normally taken to be that due to the transfer of energy by radiation in the diffusion approximation, was redefined to permit  $\beta$  cooling. As in Boss (2017, 2019), the values of  $\beta$  that were explored (see Table 1) were 1, 3, 10, 20, 30, 40, 50, and 100.

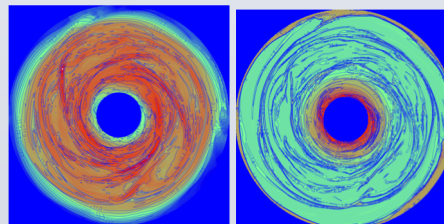
## Midplane Density (L) and Temperature (R) for Varied Beta



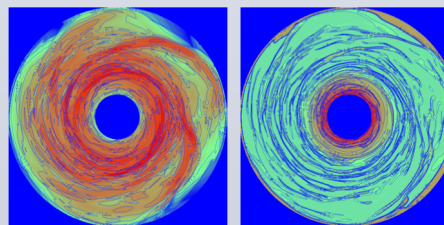
Beta = 1



Beta = 10



Beta = 30



Beta = 100

## New Results

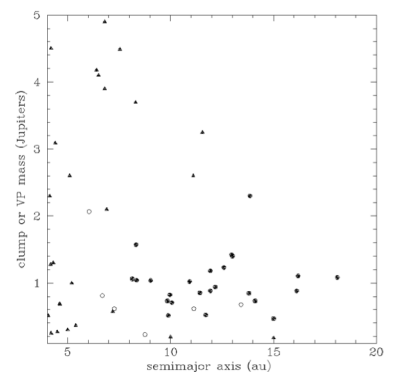
The new models were started from the last saved time step of the model with corresponding  $\beta$  in Boss (2019) before VPs were inserted, i.e., when the grids had only been doubled in  $r$  and  $\phi$ , but not yet quadrupled. Table 1 lists the key results for all of the models: the final times reached, the number of VPs and clumps present at the final time, the sum of those two ( $N_{VP} + N_{clumps} = N_{total}$ ), and the number of VPs in Boss (2019) at the time step closest to the final time of the new models. The number of clumps ( $N_{clumps}$ ) was assessed by searching for dense regions with densities greater than  $10^{18} \text{ g cm}^{-3}$ . For clumps of this density or higher, the free fall time is 6.7 yrs or less, considerably less than the orbital periods. The orbital period of the disk gas at the inner edge (4 au) is 8.0 yr and 91 yrs at the outer edge (20 au). The final times reached ranged from 205 yrs to 326 yrs, indicating that the models spanned time periods long enough for many revolutions in the inner disk and multiple revolutions in the outer disk. Each model required about 2.5 years of time to compute, each running on a separate, single core of the Carnegie memex cluster at Stanford University.

## Results for Quadrupled Grid Models Compared to VP Models

Table 1. Results for the new models with varied  $\beta$  cooling and quadrupled spatial resolution, showing the number of VPs and clumps at the final time, the sum of those two ( $N_{VP} + N_{clumps} = N_{total}$ ), and the number of VPs in Boss (2019) at the time step closest to the final time of the new models.

Model	$\beta$	final time (yrs)	$N_{VP}$	$N_{clumps}$	$N_{total}$	$N_{VP-2019}$
beq1	1	210	0	4	4	5
beq2	3	296	0	4-6	4-6	4
beq3	10	223	1	3-5	4-6	3
beq4	20	267	0	0-1	0-1	2
beq5	30	205	0	1-2	1-2	3
beq6	40	245	0	0-3	0-3	1
beq7	50	306	0	1-2	1-2	1
beq8	100	326	0	2	2	2

## Clump masses (filled circles) compared to known exoplanet masses (filled triangles) and to VP masses (open circles) of Boss (2019) at same time as clumps in quadrupled models.



Boss, A. P. 2017, ApJ, 836, 53

Boss, A. P. 2019, ApJ, 884, 56

Boss, A. P., & Myhill, E. A. 1992, ApJS, 83, 311